Theme 5: Physical and numerical modelling

Geotechnical Aspects of Underground Construction in Soft Ground – Ng, Huang & Liu (eds)
© 2009 Taylor & Francis Group, London, ISBN 978-0-415-48475-6

Tunnel behaviour under seismic loads: Analysis by means of uncoupled and coupled approaches

D. Boldini
Department of Chemical, Mining and Environmental Engineering, University of Bologna, Bologna, Italy

A. Amorosi
Department of Civil and Environmental Engineering, Technical University of Bari, Bari, Italy

ABSTRACT: In this paper different approaches to investigate the behaviour of tunnel under seismic loads are presented. They include one-dimensional (1D) numerical analyses performed modelling the soil as a single phase non-linear visco-elastic medium, the results of which are then used to evaluate the input data for selected analytical solutions proposed in the literature (uncoupled approach), and 2D fully coupled Finite Element (FEM) simulations adopting a visco-elastic effective stress model for the soil (coupled approach).

1 INTRODUCTION

The dynamic response of tunnels to seismic actions can be assessed by means of uncoupled or coupled approaches, depending on whether the evaluation of the seismic wave propagation and of the corresponding actions on the structure is undertaken in two separated steps or in one single analysis, respectively.

In this paper the transverse seismic behaviour of an idealised shallow tunnel in soft clay is analysed by means of uncoupled and coupled approaches. They include one-dimensional (1D) numerical analyses performed modelling the soil as a single phase non-linear visco-elastic medium and 2D fully coupled Finite Element (FEM) simulations adopting a visco-elastic effective stress model for the soil.

In the uncoupled approach 1D visco-elastic analyses, performed using the equivalent linear scheme implemented in the code EERA (Bardet et al. 2000), are aimed at establishing the role of stiffness and damping non-linearity on the free-field site response. The results of the analyses at the tunnel depth are then used to evaluate the input data for selected analytical solutions proposed in the literature to predict the transverse response of the structure both for full-slip and no-slip conditions (e.g., Wang 1993). This approach, widely used in the engineering practice, is based on the assumptions that the free-field site response is representative of the problem under study and that the seismic event at the tunnel depth can be satisfactorily represented by means of the maximum shear strain induced in the soil and the corresponding mobilised stiffness.

To overcome some of the limitations of the approach described above a fully coupled Finite Element analysis can be adopted, simulating in the time domain the soil-structure dynamic interaction during the seismic event. This latter is in this case realistically described by an accelerogram and the soil by an appropriate effective stress formulation.

The constitutive assumption for the soil is a key element of this class of analyses. A linear visco-elastic model is often adopted at the scope, for its apparent simplicity and limited number of parameters. In fact, a number of commercial codes nowadays allow the user to perform coupled dynamic analyses based on linear elasticity and viscous damping, this latter accounted for by the Rayleigh formulation. In this case a limitation of the coupled approach is in the non obvious selection of adequate elastic and viscous soil parameters, which sensibly influence the results of the analysis.

In this work a strategy to calibrate the parameters for the visco-elastic model adopted in the FEM analyses is proposed based on the free field soil response results obtained in the context of the uncoupled approach.

A critical comparison between coupled and uncoupled approaches is outlined in the paper with reference to a shallow tunnel excavated by a TBM. A realistic geotechnical characterisation is assumed for the idealised soft clay deposit under study.

2 CASE STUDY

In the present study the acceleration time history recorded at Kalamata (Greece) during the 13.XI.1986 earthquake is considered. The original seismic signal is characterised by a duration of 29.74 s and a maximum acceleration of 0.24 g.

The input signal adopted in this work was scaled at 0.35 g and was filtered to prevent frequency levels higher than 7 Hz. A picture of the selected acceleration time history after manipulation is given in Figure 1 while the resulting Fourier spectrum is shown in Figure 2.

In all the analyses the seismic signal is assumed to be applied at the outcrop of the deposit. The corresponding bedrock motion was calculated by means of a deconvolution analysis performed by the code EERA, as described in the next paragraph.

A 60-m thick ideal deposit of soft clay is assumed as the reference soil profile, characterised by the following physical and mechanical parameters: plasticity index $IP = 44\%$, unit weight of volume $\gamma = 17\ \text{kN/m}^3$, overconsolidation ratio in terms of mean effective stress $R = 1.5$, small strain shear stiffness $G_O =$ variable with depth, Poisson's ratio $\upsilon' = 0.25$, damping ratio $D =$ variable with depth, coefficient at rest $K_0 = 0.6$. The water table is assumed at the ground surface.

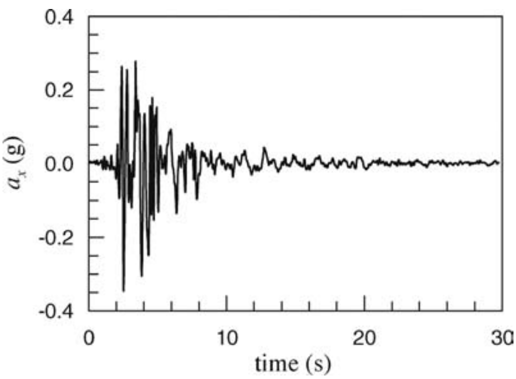

Figure 1. Modified acceleration time history scaled at 0.35 g.

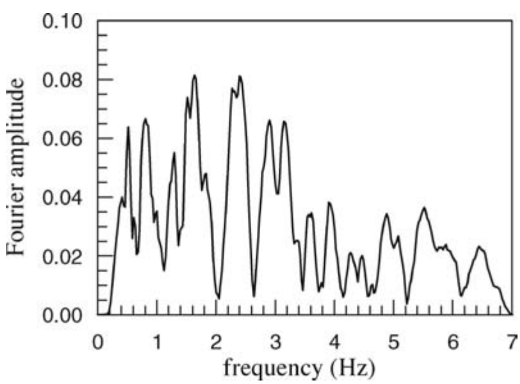

Figure 2. Frequency-filtered Fourier spectrum.

A circular tunnel, located at a depth of 15 m and characterised by a 10.10 m diameter is selected as the reference underground structure for the present study. The lining is assumed to be composed by 0.50 m thick precast concrete segments characterised by the following parameters: Young's modulus $E_l = 38$ GPa, Poisson's ratio $\nu_l = 0.25$, damping ratio $D_l = 5\%$.

3 UNCOUPLED APPROACH

The 1D ground response analysis was performed with the code EERA (Bardet et al. 2000) that analyses the vertical propagation of shear waves in a one-dimensional layered system based on an equivalent-linear visco-elastic scheme. It assumes that the shear modulus G and damping ratio D are function of shear strain amplitude γ.

The adopted profile of the small-strain shear stiffness G_O with depth (Figure 3) was evaluated by the relationship proposed by Viggiani (1992) as a function of the in situ mean stress, R and IP.

Figure 4 shows the curves of the variation of the normalised shear stiffness and damping ratio with shear strain γ, defined according to Vucetic & Dobry (1991).

A total number of 31 layers was adopted to discretise the soil stratum.

Figure 5 shows the results of the analysis in terms of maximum shear strain γ_{max}, normalised shear stiffness G/G_O, damping ratio D and maximum acceleration a_{max} with depth.

Values of γ_{max} and G obtained at the depth of 15 m, i.e. at the tunnel depth, were subsequently used

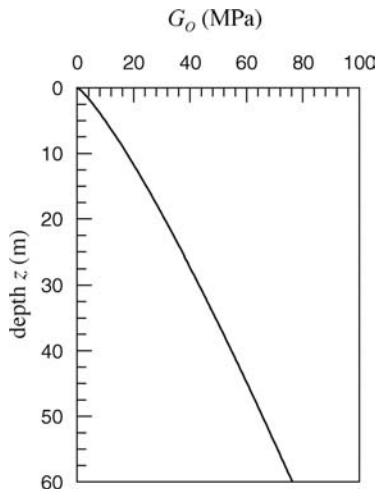

Figure 3. Profile of the small-strain shear stiffness G_O.

to evaluate the increment of hoop forces and bending moments acting on the tunnel lining during the earthquake, according to selected analytical solutions proposed in the literature.

Here, the solutions proposed by Wang (1993) to predict the response of the structure are taken into consideration for both full-slip and no-slip conditions.

The maximum increment of hoop force and bending moment in the transverse direction of the tunnel are given by:

$$\Delta N_{max} = \pm\frac{1}{6}K_1\frac{E_u}{(1+\nu_u)}r\gamma_{max} \tag{1}$$

$$\Delta M_{max} = \pm\frac{1}{6}K_1\frac{E_u}{(1+\nu_u)}r^2\gamma_{max} \tag{2}$$

for full-slip conditions and by:

$$\Delta N_{max} = \pm K_2\frac{E_u}{2(1+\nu_u)}r\gamma_{max} \tag{3}$$

for no-slip conditions, the bending moment being the same for the two cases. E_u and ν_u indicate the

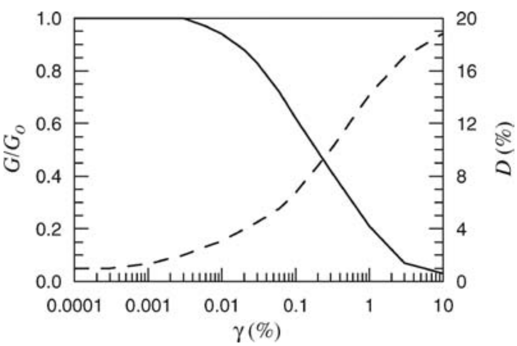

Figure 4. Modulus reduction curve G/G_O and variation of damping ratio D with shear strain γ.

mobilised soil Young's modulus (evaluated with reference to the previously calculated mobilised shear modulus G) and the Poisson's ratio (assumed equal to 0.5) in undrained conditions, respectively. r is the tunnel radius. K_1 and K_2 are given by the following expressions:

$$K_1 = \frac{12(1-\nu_u)}{2F+5-6\nu_u} \tag{4}$$

$$K_2 = 1+\frac{F\left[(1-2\nu_u)-(1-2\nu_u)C\right]-\frac{1}{2}(1-\nu_u)^2+2}{F\left[(3-2\nu_u)+(1-2\nu_u)C\right]+C\left[\frac{5}{2}-8\nu_u+6\nu_u^2\right]+6-8\nu_u} \tag{5}$$

where:

$$C = \frac{E_u\left(1-\nu_l^2\right)r}{E_l\,t\,(1+\nu_u)(1-2\nu_u)} \tag{6}$$

$$F = \frac{E_u\left(1-\nu_l^2\right)r^3}{6E_l I(1+\nu_u)} \tag{7}$$

are the compressibility and flexibility ratios and t and I the thickness and the moment of inertia of the tunnel lining, respectively.

Table 1 summarises the computed increments of hoop force and bending moment for both full-slip and no-slip conditions.

4 COUPLED APPROACH

The coupled analyses were performed by the Finite Element commercial code PLAXIS, which describes

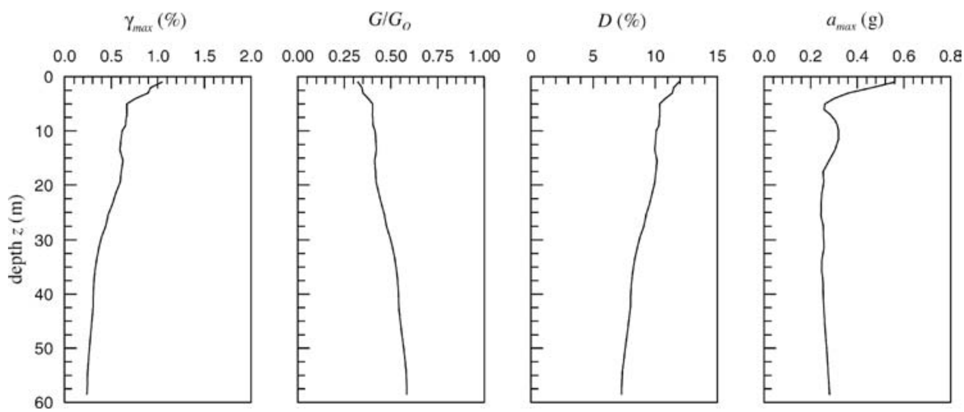

Figure 5. Results of the 1D ground response analysis performed with EERA.

Table 1. Increments of hoop force and bending moment according to Wang (1993).

Full-slip conditions		No-slip conditions	
ΔN_{max} (kN/m)	ΔM_{max} (kNm/m)	ΔN_{max} (kN/m)	ΔM_{max} (kNm/m)
±159	±802	±473	±802

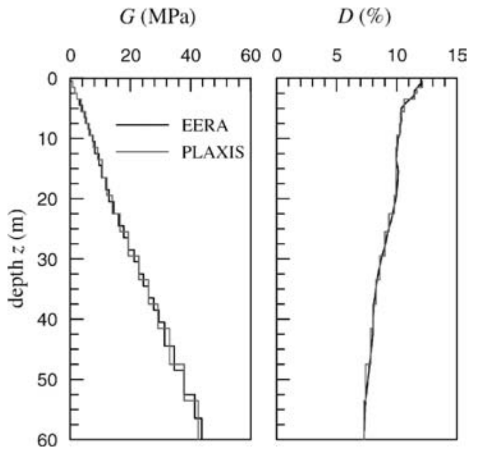

Figure 6. Calibration of the G and D profiles assumed in the FEM analyses on the basis of EERA results.

the mechanical behaviour of the soil in terms of effective stress.

In order to perform a comparative analysis with the EERA results a linear visco-elastic constitutive model was selected. In the constitutive model viscous damping was accounted for by the Rayleigh formulation.

4.1 *Calibration of the visco-elastic parameters*

The constitutive model employed in the FEM analyses makes use of constant-value elastic and viscous parameters for each sub-layer of the discretised deposit. In this respect, it is of paramount importance to define appropriate values of these parameters as a function of the strain level attained in the soil deposit during the earthquake.

In this paper a recently developed calibration procedure of the visco-elastic parameters to be assumed in dynamic FEM analyses is adopted (Amorosi et al. 2007). G and D profiles are set in such a way to match the corresponding profiles obtained by the free-field EERA analysis. To this end the numerical model is divided into a relatively large number of sub-layers in order to obtain an as close as possible correspondence (Figure 6).

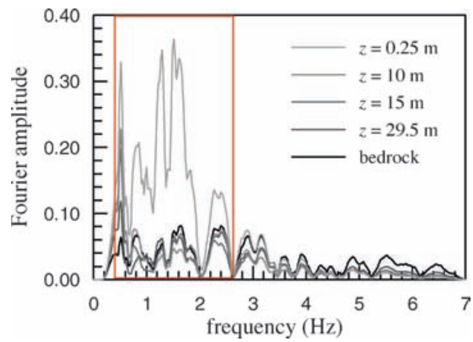

Figure 7. Fourier spectra computer by EERA at different depths and high-energy frequency interval.

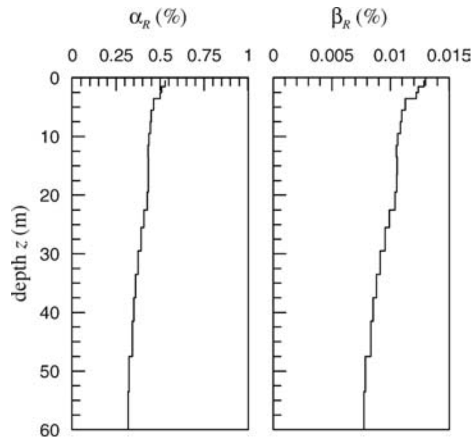

Figure 8. α_R e β_R profiles assumed in the FEM analyses on the basis of EERA results.

The profiles of the Rayleigh coefficients α_R e β_R are obtained correspondingly, according to the following relationship with the damping ratio D (e.g., Clough & Penzien 2003):

$$\begin{Bmatrix} \alpha_R \\ \beta_R \end{Bmatrix} = \frac{2D}{\omega_n + \omega_m} \begin{Bmatrix} \omega_n \omega_m \\ 1 \end{Bmatrix} \quad (8)$$

where ω_n e ω_m are the circular frequencies related to the cyclic frequency interval $f_n \div f_m$. The frequency range was determined by selecting the interval where the Fourier spectra computed by EERA at different depths were characterised by the highest energy content (indicated in the box of Figure 7). The resulting α_R e β_R profiles are shown in Figure 8.

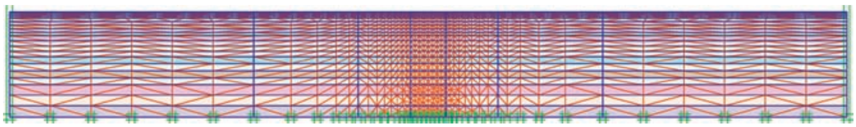

Figure 9. Mesh employed in the FEM analyses.

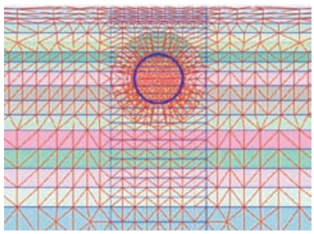

Figure 10. Detail of the mesh around the tunnel section.

4.2 *Numerical model*

The dimension and boundary conditions of the 2D FEM numerical model were set up after a considerable number of preliminary analyses performed to minimise the influence of boundary conditions on the computed results.

The mesh employed in the present study is reported in Figure 9: it is characterised by a width equal to 8 times its height. The base is assumed to be rigid and at the lateral sides the viscous boundaries proposed by Lysmer & Kuhlmeyer (1969) were used.

The domain was discretised in 2431 15-node plane strain triangular elements. In the central part of the mesh, where the tunnel is located, the element dimension h always satisfies the condition:

$$h \le h_{max} = V_S / (6 \div 7) f_{max} \qquad (9)$$

where V_S is the shear wave velocity and f_{max} is the maximum frequency of the seismic signal.

A detail of the mesh around the tunnel is shown in Figure 10.

The following stages were simulated in the numerical analysis:

- first, the tunnel was excavated in undrained conditions imposing a volume loss of 0.4%;
- next, the lining was installed and the post-excavation consolidation phase was studied;
- the select seismic signal was then applied at the bottom of the model in undrained conditions.

In all the static stages of the analysis the soil stiffness for each sub-layer was selected scaling down the value of the very small strain shear stiffness G_O by a factor of 0.45 to account for an average shear strain level involved in the excavation stages of $\overline{\gamma} = 0.1\%$.

An interface was activated between the soil and the lining, characterised by a normal and tangent stiffness corresponding to that of the adjacent soil: such a condition can be considered similar to the so-called no-slip conditions of the Wang's solutions.

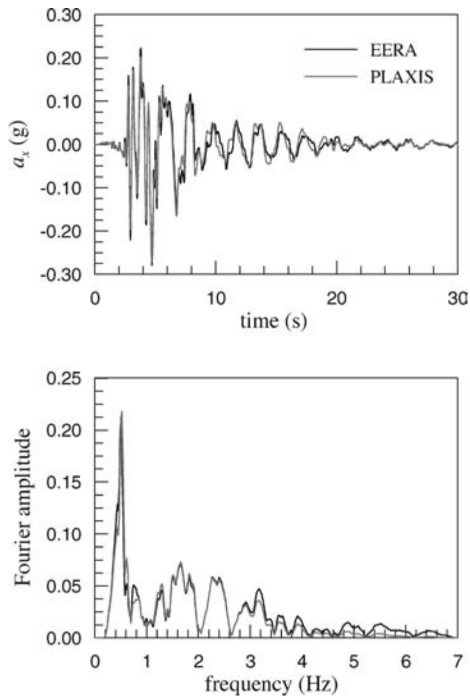

Figure 11. Comparison between EERA and PLAXIS free-field soil response analyses at 15 m depth.

4.3 *Free-field soil response results*

In this paragraph a preliminary comparison between free-field soil response results at the tunnel depth is provided to check the consistency between the 1D and 2D proposed approaches. In this case the 2D model does not incorporate the tunnel and, as such, the result can be directly compared to that of the corresponding 1D free-field analysis.

Figure 11 shows the acceleration time histories and the Fourier spectra computed by EERA and PLAXIS. A satisfactory agreement is obtained between the two solutions, demonstrating the effectiveness of the proposed calibration strategy.

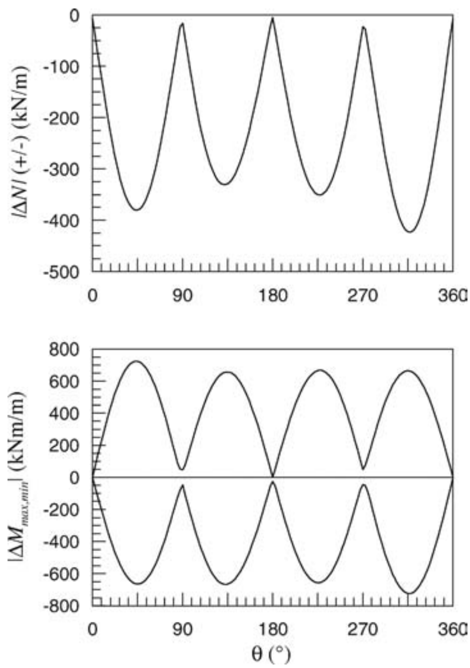

Figure 12. Increments of hoop force and bending moment during the seismic event.

4.4 *Results of the coupled analyses*

The maximum increment of the seismic-induced absolute hoop forces and positive and negative bending moments in the tunnel lining were computed by the 2D FEM coupled analyses and are represented in Figure 12. The results are reported as a function of the angle θ indicated in Figure 12 and defined positive in counter-wise direction.

Results indicate a satisfactory match between the maximum increments of hoop force and bending moments predicted by the visco-elastic FEM solution ($\Delta N_{max} = \pm 423$ kN/m e $\Delta M_{max} = \pm 724$ kNm/m) and those resulting from the Wang's solutions for the no-slip case.

5 CONCLUSIONS

In this paper the transverse dynamic response of a shallow tunnel subjected to seismic actions is investigated by means of uncoupled and coupled approaches.

The former approach, traditionally used in the engineering practice, combines a free-field site response analysis with a set of analytical solutions to evaluate the maximum increment of hoop force and bending moment in the tunnel lining. This approach is based on a limited numbers of parameters to describe the earthquake, the soil behaviour and thawt of the tunnel lining. The reliability of the uncoupled approach is supported by the satisfactory performance of a number of underground structures designed based on it.

Nowadays the availability of relatively sophisticated commercial FEM codes and the continuous increase in computational power allows to approach the same problem by means of a single analysis which, at the same time, accounts for the seismic site response, the soil-structure interaction and the actions in the tunnel lining. This coupled approach is characterised by a far more detailed description of the seismic actions at the tunnel depth as compared to the uncoupled one and allows to describe the soil behaviour by means of effective stress based constitutive models. Concerning this last feature in this paper a simple assumption was made: linear visco-elasticity was assumed for the clayey deposit under study, where viscous damping was accounted for by the Rayleigh formulation. Although very simple this constitutive assumption already poses some problems in the calibration of the stiffness and Rayleigh damping parameters. In fact, it is a well established fact that the profiles of these parameters with depth crucially influence the results of any FEM dynamic analysis (e.g.: Woodward & Griffiths 1996). Related to this, a strategy for the calibration of the stiffness and Rayleigh damping parameters is proposed in the paper. The results of the coupled analysis based on this calibration satisfactory match those obtained by the uncoupled approach in terms of hoop force and bending moments in the lining.

In the Authors' opinion this encouraging result represents a necessary condition to extend the use of the proposed calibration strategy to the case of more complex constitutive assumptions including plasticity.

REFERENCES

Amorosi, A., Boldini, D., Elia, G., Lollino P. & Sasso M. 2007. Sull'analisi della risposta sismica locale mediante codici di calcolo numerici. *IARG 2007*, Salerno.

Bardet, J.P., Ichii, K. & Lin C.H. 2000. *EERA-A computer program for Equivalent-linear Earthquake site Response Analyses of layered soils deposits*. User Manual.

Clough, R. & Penzien, J. 2003. *Dynamics of Structures*. Computers and Structures Inc.

Lysmer, J.& Kuhlemeyer, R.L. 1969. Finite dynamic model for infinite media. *ASCE EM* 90: 859–877.

PLAXIS. 2003. *Reference Manua*l, version 8.

Viggiani, G.M.B. 1992. *Small strain stiffness of fine grained soils*. PhD thesis. City University. London.

Vucetic, M. & Dobry, R. 1991. Effects of the soil plasticity on cyclic response. *Journal of Geotech. Eng. Div., ASCE* 117(1): 89–107.

Wang, J.N. 1993. *Seismic design of tunnels: a state-of-the-art approach*. Monograph 7, Parsons, Brinckerhoff, Quade & Diuglas Inc., New York.

Woodward, P.K. & Griffiths, D.V. 1996. Influence of viscous damping in the dynamic analysis of an earth dam using simple constitutive models. *Computers and Geotechnics* 19(3): 245–263.